RIG-I–like receptor LGP2 protects tumor cells from ionizing radiation

Ryan C. Widau[a,1], Akash D. Parekh[a,1], Mark C. Ranck[a,1], Daniel W. Golden[a,1], Kiran A. Kumar[a], Ravi F. Sood[a], Sean P. Pitroda[a], Zhengkai Liao[a], Xiaona Huang[a], Thomas E. Darga[a], David Xu[a], Lei Huang[b], Jorge Andrade[b], Bernard Roizman[c,2,3], Ralph R. Weichselbaum[a,2], and Nikolai N. Khodarev[a,2]

[a]Department of Radiation and Cellular Oncology and Ludwig Center for Metastasis Research, [b]Center for Research Informatics, and [c]The Marjorie B. Kovler Viral Oncology Laboratories, University of Chicago, Chicago, IL 60637

Contributed by Bernard Roizman, December 13, 2013 (sent for review November 13, 2013)

An siRNA screen targeting 89 IFN stimulated genes in 14 different cancer cell lines pointed to the RIG-I (retinoic acid inducible gene I)–like receptor Laboratory of Genetics and Physiology 2 (LGP2) as playing a key role in conferring tumor cell survival following cytotoxic stress induced by ionizing radiation (IR). Studies on the role of LGP2 revealed the following: (*i*) Depletion of LGP2 in three cancer cell lines resulted in a significant increase in cell death following IR, (*ii*) ectopic expression of LGP2 in cells increased resistance to IR, and (*iii*) IR enhanced LGP2 expression in three cell lines tested. Studies designed to define the mechanism by which LGP2 acts point to its role in regulation of IFNβ. Specifically (*i*) suppression of LGP2 leads to enhanced IFNβ, (*ii*) cytotoxic effects following IR correlated with expression of IFNβ inasmuch as inhibition of IFNβ by neutralizing antibody conferred resistance to cell death, and (*iii*) mouse embryonic fibroblasts from IFN receptor 1 knockout mice are radioresistant compared with wild-type mouse embryonic fibroblasts. The role of LGP2 in cancer may be inferred from cumulative data showing elevated levels of LGP2 in cancer cells are associated with more adverse clinical outcomes. Our results indicate that cytotoxic stress exemplified by IR induces IFNβ and enhances the expression of LGP2. Enhanced expression of LGP2 suppresses the IFN stimulated genes associated with cytotoxic stress by turning off the expression of IFNβ.

innate immunity | cytoplasmic sensor | interferon beta | DHX58

Several studies have shown that the response of tumor cells to ionizing radiation (IR) is associated with IFN-mediated signaling (1–6). IFN signaling leads to the induction of multiple IFN stimulated genes (ISGs) (7, 8) and activates growth arrest and cell death in exposed cell populations (9). The precise mechanism of IR-mediated induction of IFN signaling is unknown. Tumor cell clones that survive an initial cytotoxic insult are subsequently resistant to exposure to both IR and prodeath components of IFN signaling (10). These clones express IFN-dependent enhanced levels of constitutively expressed ISGs, which overlap in part with ISGs initially induced by cytotoxic stress. Many of these constitutively expressed ISGs have been characterized as antiviral genes (11). Recently, enhanced levels of constitutively expressed ISGs have been reported in advanced cancers and were often associated with a poor prognosis related to aggressive tumor growth, metastatic spread, resistance to IR/chemotherapy, or combinations of these factors (11–18). The studies presented in this report are based on the hypothesis that a specific set of constitutively expressed ISGs, whose enhanced expression is by cytotoxic stress, confers a selective advantage to individual tumor clones (5, 9, 10, 13, 19).

To test this hypothesis, we designed a targeted siRNA screen against 89 ISGs selected from two sources. The first included ISGs identified in our earlier screen and designated the IFN-Related DNA Damage Signature (IRDS) (1, 13). The second set included related ISG signatures that have been reported in the literature (as described in *Methods* and Dataset S1). The 89 genes were individually targeted in 14 tumor cell lines derived from malignant gliomas, lung, breast, colon, head and neck, prostate, and bladder cancers.

The most significant finding from this screen was that the RNA helicase Laboratory of Genetics and Physiology 2 (LGP2) encoded by DHX58 [DEXH (Asp-Glu-X-His) box polypeptide 58] confers survival and mediates the response to IR of multiple tumor cell lines. LGP2 acts as a suppressor of the RNA-activated cytoplasmic RIG-I RIG-I (retinoic acid inducible gene I)–like receptor's pathway (20, 21). This pathway is a subtype of pattern recognition receptors responsible for primary recognition of pathogen and host-associated molecular patterns and the subsequent activation of type I IFN production that orchestrates an innate immune response (22–24). In addition to its role in inhibiting IFNβ expression, Suthar et al. recently demonstrated that LGP2 governs CD8+ T-cell fitness and survival by inhibiting death-receptor signaling (25). Here we demonstrate that suppression of LGP2 leads to an enhanced IFNβ expression and increased killing of tumor cells. Our results thereby provide a mechanistic connection between IR-induced cytotoxic response in tumor cells and the LGP2–IFNβ pathway.

Results

Expression of LGP2 Is Associated with Tumor Cell Survival. On the basis of our earlier studies (1, 2, 13, 26), we hypothesized the existence of ISGs that are constitutively expressed in aggressive cancers and confer prosurvival functions following cytotoxic stress caused by DNA-damaging agents. To identify the key members of this group, we compiled a list of ISGs associated

Significance

An undesirable outcome of radiotherapy (ionizing radiation, IR) of cancer is the emergence of radioresistant cells. We report that Laboratory of Genetics and Physiology 2 (LGP2), a resident RIG-I (retinoic acid inducible gene I)–like receptor protein, can induce radioresistance. IR induces interferon and stimulates accumulation of LGP2. In turn, LGP2 shuts off the synthesis of interferon and blocks its cytotoxic effects. Ectopic expression of LGP2 enhances resistance to IR, whereas depletion enhances cytotoxic effects of IR. Here we show that LGP2 is associated with radioresistance in numerous diverse cancer cell lines. Examination of available databases links expression of LGP2 with poor prognosis in cancer patients.

Author contributions: R.C.W., D.W.G., R.F.S., S.P.P., B.R., R.R.W., and N.N.K. designed research; R.C.W., A.D.P., M.C.R., D.W.G., K.A.K., R.F.S., S.P.P., Z.L., X.H., T.E.D., and D.X. performed research; R.C.W., A.D.P., M.C.R., D.W.G., K.A.K., R.F.S., S.P.P., Z.L., L.H., J.A., B.R., R.R.W., and N.N.K. analyzed data; and R.C.W., B.R., R.R.W., and N.N.K. wrote the paper.

The authors declare no conflict of interest.

[1]R.C.W., A.D.P., M.C.R., and D.W.G. contributed equally to this work.

[2]B.R., R.R.W., and N.N.K. contributed equally to this work.

[3]To whom correspondence should be addressed. E-mail: bernard.roizman@bsd.uchicago.edu.

This article contains supporting information online at www.pnas.org/lookup/suppl/doi:10.1073/pnas.1323253111/-/DCSupplemental.

with aggressive tumors from multiple published studies (Dataset S1). In total, 89 genes were selected for further evaluation based on either inclusion in the IRDS (13) or inclusion in at least two reported ISG-related signatures (Dataset S1 and Dataset S2). To test whether expression of these genes conferred a survival advantage to tumor cells, we performed a targeted siRNA screen in a panel of 14 cell lines consisting of two lung cancer, three high-grade glioma, three breast cancer and normal breast epithelium, two colon cancer, two head and neck cancer, one bladder cancer, and one prostate cancer cell lines. Each tumor cell line, both untreated and after exposure to 3 Gy, was targeted with pooled siRNAs against each of the selected 89 genes and scored on the basis of cell viability. To identify genes with prosurvival functions common across multiple cell lines tested, we used a rank aggregation approach assuming each cell line was an independent dataset (27, 28). With different modes of normalizations and perturbations, LGP2 was invariably the top ranked gene in unirradiated cells (Fig. 1). In addition, LGP2 was among the top ranked genes conferring survival to multiple cancer cell lines after irradiation at 3 Gy. The focus of this report is on the role of LGP2 in the regulation of cell survival.

LGP2 Blocks Apoptosis Induced by IR. The desirable endpoint of radiotherapy is induction of apoptosis in irradiated cells. To define the role of LGP2 in determination of the outcome of IR treatment, we tested the effects of depletion of LGP2 on induction of apoptosis by IR in WiDr (colorectal adenocarcinoma), D54 (glioblastoma), and Scc61 (head and neck squamous cell carcinoma) cancer cell lines. As detailed in *Methods* and in the figure legends, the cell lines were transfected with nontargeted (scrambled) siRNA (siNT) or targeted (siLGP2) siRNA and either mock-irradiated or irradiated (5 Gy) 24 h after transfection. The cells were stained with Annexin V and propidium iodide and scored for both markers by flow cytometry 48 h after IR or mock treatment. The results were as follows.

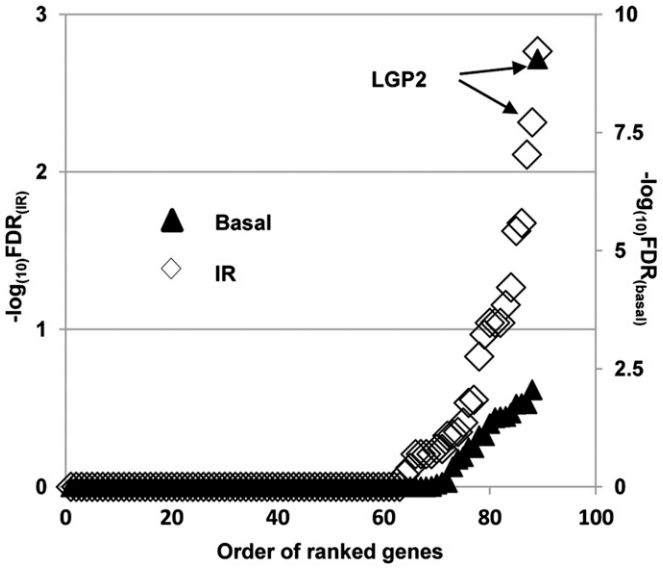

Fig. 1. Identification of LGP2 as prosurvival ISG. In each cell line tested, 89 screened genes were ranked according to the ability of corresponding siRNAs to suppress cell viability as measured by CellTiter-Glo luminescent assay (Promega). FDR-corrected significance values for each gene across all tested cell lines were estimated by rank aggregation approach (*Methods*). Data are presented as negative log-transformed FDRs for each gene on the basal level (closed triangles, right *y* axis) and 48 h after irradiation at 3 Gy (open diamonds, left *y* axis).

As shown in Fig. 2*A* and in Fig. 2*B*, transfection of WiDr cells with a siNT led to a small (4.66%) increase in double-positive cells (Fig. 2 *A*, *a*), whereas 73.7% of the cell population remained viable under these conditions (Fig. 2 *A*, *b*). Irradiation of siNT-transfected cells led to an approximately twofold increase in cell death (9.8%) with an 8.6% reduction in viable cells (65.1%) (Fig. 2 *A*, *c* and *d*, respectively). Suppression of LGP2 alone led to an increase in double-positive cells to 37.9% (8.1-fold increase) (Fig. 2 *A*, *e*). The combination of LGP2 suppression followed by irradiation led to further accumulation of double-positive cells to 56.6%, a 12.1-fold increase relative to the nonirradiated siNT control (Fig. 2 *A*, *f*).

Similar data were obtained with D54 and Scc61 cells (Fig. 2*B*). As shown in Fig. 2*B*, *Left*, siRNA knockdown of LGP2 in the D54 cells led to a fourfold increase in cell death at baseline and a 7.5-fold increase following irradiation. The same conditions led to 6.4-fold cell death at baseline and 10-fold induction following IR in the WiDr cell line (Fig. 2*B*, *Left*). A similar pattern was found in the Scc61 cell line (Fig. 2*B*, *Right*; $P < 0.05$). Clonogenic survival analyses revealed that siRNA-mediated depletion of LGP2 reduced radioresistance in both D54 and Scc61 cell lines. Compared with siNT control, irradiation of LGP2-depleted cells lead to 4.7-fold decrease in the survival fraction in D54 cells ($P = 0.014$) and a 20.3-fold decrease in the survival fraction of Scc61 cells ($P = 0.00056$) at 7 Gy (Fig. 2 *C* and *D*, respectively). We conclude that suppression of LGP2 results in apoptosis and radiosensitization.

Overexpression of LGP2 Protects Cells from IR. To verify the conclusion that LGP2 protects tumor cells from the cytotoxic effects of radiotherapy, we investigated the clonogenic survival of tumor cells expressing the full-length cDNA of LGP2. In this experiment, D54 cells were stably transfected with the plasmid p3xFLAG-cytomegalovirus 10 (CMV10)–LGP2 encoding LGP2 or control p3xFLAG–CMV10 (Flag). Positive clones were plated in six-well plates and exposed to 0, 5, or 7 Gy. The amounts of LGP2 protein in mock- (Flag) transfected and LGP2-transfected cells are shown in Fig. 3*B*, *Inset*. Fig. 3*A* shows the surviving cell colonies stained with crystal violet 12 d after irradiation. Fig. 3*B* shows the fraction of mock-transfected and LGP2-transfected cells that survived exposure to IR quantified as described in *Methods*. We conclude that ectopic expression of LGP2 confers increased resistance to IR.

IR Induces Expression of LGP2. We next asked if exposure to IR would up-regulate LGP2 expression in tumor cells. In this experiment, D54, Scc61, and WiDr cells were mock-treated or exposed to 6 Gy. The cells were harvested 72 h after IR, solubilized, and tested for the presence of LGP2 by immunoblotting with anti-LGP2 antibody; actin served as loading control. As shown in Fig. 4, a significant increase in LGP2 expression was observed in IR-treated cells. We conclude that IR induces the expression of LGP2.

IR Induces Cytotoxic Type I IFN. LGP2 functions to suppress type I IFN production in response to viral infection or transfection of double-stranded RNA mimetics (21, 29–32). The objective of the studies described in this section was to determine whether IR induces a type 1 IFN response. In these studies, D54, WiDr, Scc61, or HEK293 cells were mock-treated or exposed to 6 Gy. The cells were harvested 72 h after IR, and IFNβ expression relative to GAPDH was determined by real-time PCR. As shown in Fig. 5*A*, exposure to IR increased the relative expression of IFNβ mRNA in D54, WiDR, SCC61, and HEK293 cell lines by 58-, 42-, 12-, and 28-fold, respectively. In a complementary approach, we investigated the ability of IR to activate a plasmid reporter under the control of IFNβ promoter (IFNβ–Luc) (33). In these experiments, HEK293 cells were cotransfected with IFNβ–Luc and pRL–SV40 (*Renilla*). At 24 h after transfection,

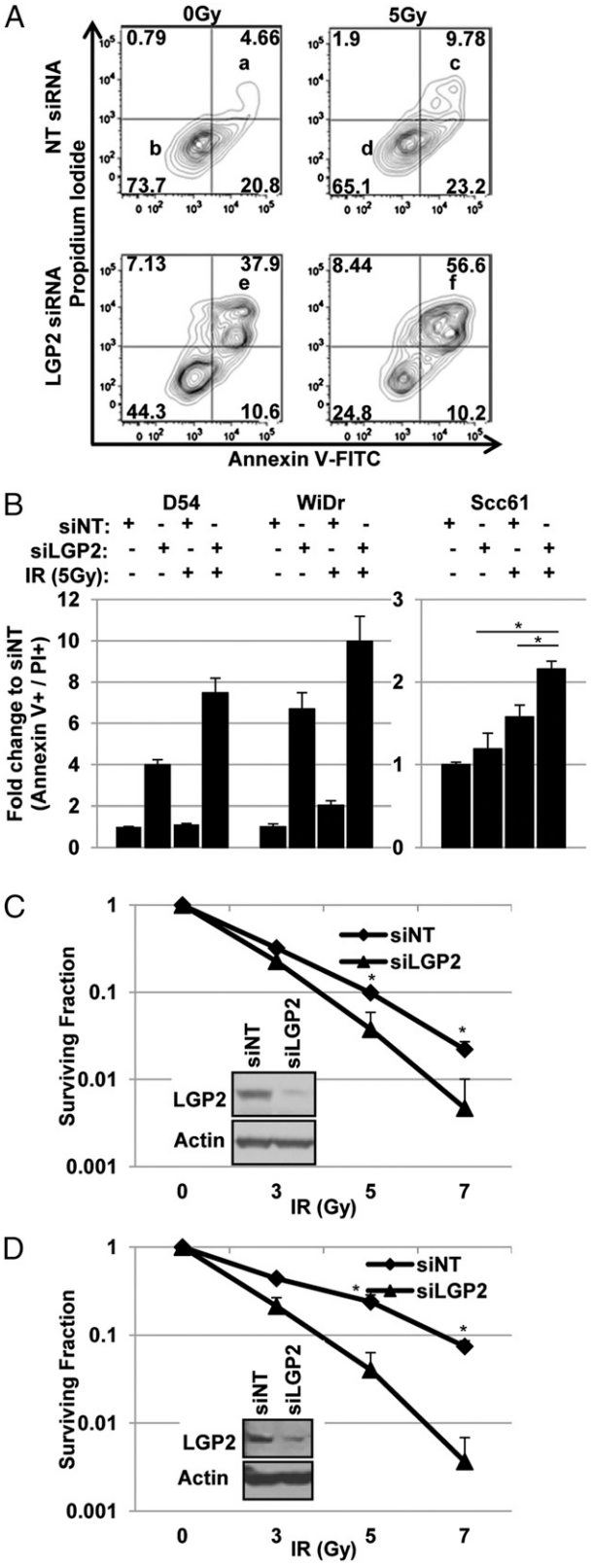

Fig. 2. Knockdown of LGP2 enhances radiation-induced killing. Cell death was quantified by flow cytometric analysis using Annexin V and propidium iodide staining. Tumor cells were treated with IR (5 Gy) 24 h posttransfection with the indicated siRNA. (*A*) Graphical representation of flow cytometric data in WiDr cells that were collected 48 h post-IR treatment. (*B*) Quantification of flow cytometric experiments in D54, WiDr, and Scc61 cells collected 48 h post-IR treatment. The data are represented as fold change relative to siNT at 0 Gy. (*C* and *D*) Clonogenic survival curves in D54 (*C*) and Scc61 (*D*) cells transiently transfected with siNT or siLGP2 and irradiated at 0, 3, 5, or 7 Gy. Data are represented in a semilog scale. Western blots are representative of siRNA-mediated knockdown of LGP2. In all experiments, data are presented as mean values of at least three independent measurements; error bars are SDs, and significance was assessed using two-tailed *t* test (*$P < 0.05$).

cells were mock-treated or exposed to 3, 6, or 12 Gy. Cells were harvested at 48, 72, or 96 h and analyzed for dual luciferase activity. As shown in Fig. 5*B*, IR activated IFNβ expression in a dose- and time-dependent manner.

To determine if induction of IFNβ by IR was cytotoxic, we determined the relative radiosensistivity of immortalized murine embryo fibroblasts (MEFs) lacking the type I IFN receptor 1 ($IFNAR1^{-/-}$) as compared with wild-type (WT) MEFs. In these experiments, $IFNAR1^{-/-}$ and WT MEFs were mock-treated or exposed to 3 or 9 Gy. Cells were assessed for viability 96 h after IR as described in *Methods*. Fig. 5*C* shows that $IFNAR1^{-/-}$ MEFs are radioresistant compared with WT MEFs. We conclude that IR induces the production of cytotoxic type I IFN.

Depletion of LGP2 Enhances IFNβ-Dependent Cytotoxicity. We next assessed the role of LGP2 in regulating the IR-induced IFNβ response. HEK293 cells were transduced with lentiviral shRNA to stably reduce the levels of LGP2 or control nontargeting (shNT). Stably transduced cells were cotransfected with IFNβ–Luc and pRL–SV40, mock-treated or exposed to 6 or 12 Gy, and collected 72 h after IR. Suppression of LGP2 led to a significant increase in IFNβ reporter activity of mock-treated and greatly increased IR-induced IFNβ (Fig. 6*A*).

We next examined whether the radiosensitizing effects of LGP2 depletion were associated with a release of cytotoxic IFNβ. In this experiment, D54 cells were incubated with neutralizing antibodies against IFNβ and mock-treated or exposed to 3 or 6 Gy; viability was assessed 96 h after IR. As shown in Fig. 6*B*, neutralizing antibodies against IFNβ partially restored viability of D54 cells with LGP2 knockdown to the level of control cells (siNT). These data are consistent with earlier studies from our laboratory demonstrating that neutralizing antibodies to IFNs partially protected human tumor xenografts from IR-mediated cytotoxicity (2). These data also indicate that IR-induced tumor cell killing is mediated, in part, by the production of autocrine IFNβ (2, 10). We conclude that LGP2 suppresses IR-induced cytotoxic IFNβ production in tumor cells.

LGP2 Expression Predicts Poor Clinical Outcomes in High-Grade Gliomas. The studies described above suggest that depletion of LGP2 increases radiosensitivity, whereas overexpression of LGP2 increases radioresistance of tumor cells. A key question is whether the results presented here are consistent with clinical experience and in particular the clinical outcomes in patients undergoing radiotherapy. Multiple studies have demonstrated an overall survival benefit for postoperative radiation therapy after surgical resection compared with surgery alone in the management of newly diagnosed glioblastoma multiforme (GBM) (34–36). In addition, the response of GBM tumors to radiation predicts the patient lifespan after treatment. In this regard, we described elsewhere that ISG expression correlated with poor overall survival in patients with GBM (15). To investigate whether LGP2 gene expression is also related to clinical outcomes in patients with GBM, we analyzed two independent GBM datasets from the Cancer Genome Atlas (CGA; http://cancergenome.nih.gov/) ($n = 382$) and the Phillips et al. study ($n = 77$) (37). In Fig. 7 *A* and *C*, the relative expression of ISGs separates each dataset into ISG-positive and ISG-negative groups. Fig. 7 *A* and *C* further demonstrates that expression of LGP2 is highly associated with expression of ISGs. To examine the association of

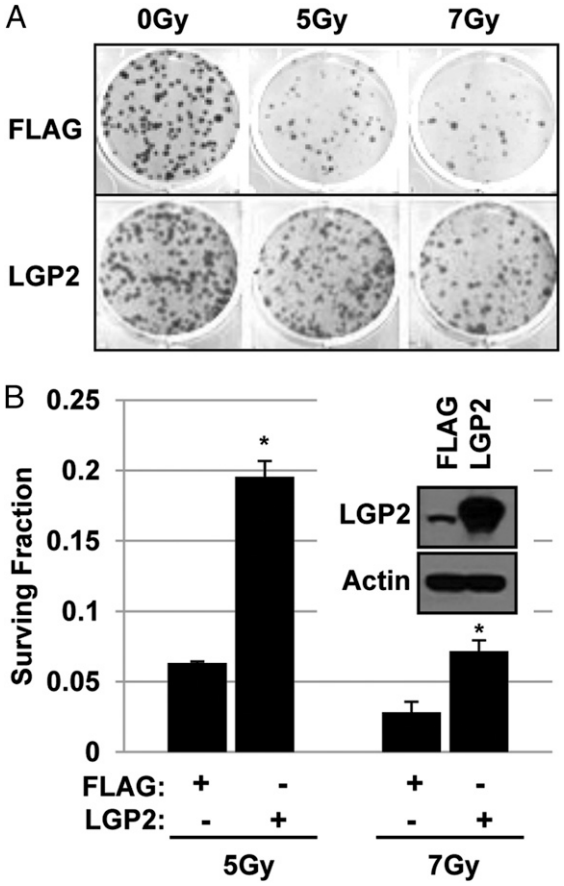

Fig. 3. Overexpression of LGP2 inhibits radiation-induced killing. D54 cells were stably transfected by full-size p3xFLAG–CMV10–LGP2 (LGP2) or control p3xFLAG–CMB10 (Flag). Selected clones were propagated, plated in six-well plates, and irradiated at 0, 5, and 7 Gy. (*A*) Crystal violet staining of survived colonies 12 d after irradiation of cells, transfected with Flag (*Upper*) or LGP2 (*Lower*). (*B*) Quantification of survival fraction of mock-transfected and LGP-transfected cells (*Methods*). Representative Western blot of stable Flag and LGP2 clone is inserted into *B*.

LGP2 expression with patient survival, we compared overall survival in the patient cohorts with relatively high and relatively low expression of LGP2. As shown in Fig. 7 *B* and *D*, high expression of LGP2 was significantly associated with a 2.3-fold increased risk for death in the Phillips et al. dataset ($P = 0.011$, Cox proportional hazards test) and a 1.4-fold increased risk for death in the CGA dataset ($P = 0.024$). These data demonstrate that LGP2 gene expression is associated with poor clinical outcomes in patients with GBM and support the notion that this protein may serve as a potential biomarker and target for the radiosensitization of high-grade gliomas.

Discussion

The salient features of the results are as follows:

i) We demonstrated a correlation between expression of LGP2 and resistance to IR in most of the 14 human cancer cell lines of diverse origins. In follow-up studies, we demonstrated that depletion of LGP2 enhanced cytotoxic sequelae of IR, whereas overexpression of LGP2 increased the fraction of cells resistant to cytotoxicity induced by IR.

ii) LGP2 is a constitutive cytoplasmic protein whose accumulation is enhanced by IFN, and hence it is defined as an ISG. Several studies have identified a link between ISGs and aggressive tumor phenotypes with poor outcomes or radio/chemoresistance (5, 10). In studies designed to explore in more detail the interaction between LGP2, IFN, and IR, we showed that IR induces both IFNβ and enhances the accumulation of LGP2, that overexpression of LGP2 causes a significant reduction of IFNβ gene expression, and lastly that inhibition of IFNβ by a neutralizing antibody results in increased resistance to cytotoxic effects induced by IR.

iii) Lastly, a survey of available databases suggests a correlation between the expression of LGP2 and poor outcomes in patients with malignant glioblastoma.

The significance of the studies presented here are as follows:

i) Expression of LGP2 emerged as necessary and on the basis of the effects of ectopic expression as sufficient for enabling enhanced survival of cancer cells exposed to cytotoxic doses of IR. Because chemotherapeutic drugs may mimic the effects of IR, LGP2 may indeed be the primary but perhaps not unique ISG to block cytotoxic manifestations associated with IFN production in cells subjected to DNA-damaging agents. Identification of the mechanism by which LGP2 acts to block IFN production may be key to development of adjunct therapies to block its function and enhance therapeutic outcomes.

ii) In light of the overwhelming evidence that LGP2 is a constitutive cellular protein whose accumulation is enhanced by IFN, the obvious question is under what conditions is LGP2 inoperative and what activates its anti-IFN functions. In principle, LGP2 acts as a classic feedback inhibitor (Fig. 8) that is activated by an unknown mechanism. The solution to this puzzle is likely to greatly accelerate the means by which its function could be blocked.

Methods

Gene Selection. We compiled 14 gene expression datasets containing ISGs in cancer cells (Dataset S1). Probe set IDs for each dataset were annotated using Ingenuity Pathway Analysis (www.ingenuity.com). Genes were included in the final screening set if they were in the IRDS or if they were reported in ≥2 other studies. After initial inclusion, all selected genes were screened in the Interferome database (www.interferome.org) to select genes activated by IFNs. In total, 89 candidate ISGs downstream from IFN/Stat were identified (Dataset S2).

siRNA Screen. siRNA screening of the selected ISGs was performed as follows. On day 1, Lipofectamine RNAiMAX diluted in Opti-MEM (Life Technologies) was added to 0.075 μL per well using a Tecan Freedom EVO 200 robotic liquid handling station to the previously prepared 384-well microplates (Corning/3712) containing immobilized individual siRNAs (Dharmacon siGENOME) plated in triplicate for each target ISG. Cells were added using a Thermo Electron MultiDrop Combi dispenser at 500 cells per well in 50 μL of RPMI 1640 media supplemented with 10% (vol/vol) FCS. The final siRNA concentration in each well was 50 nM. Plates were incubated overnight at 37 °C and on day 2 were treated with IR at a dose of 3 Gy or untreated. Plates were further incubated at 37 °C and then assayed for viability at 48 h post-IR using the highly sensitive luciferase-based CellTiterGlo assay (Promega). Luminescent reagent was added using a Thermo Electron MultiDrop Combi, and luminescent measurements were taken 90 min later using Molecular Devices Analyst GT. This platform was provided by the Cellular Screening Core, Institute for Genomics & Systems Biology, University of Chicago.

Individual siRNAs against LGP2 were validated in HCT116 and MCF10A cell lines by viability assay. Viability was assayed at 120 h posttransfection (72 h post-IR) using the the CellTiter-Glo Luminescent Cell Viability Assay

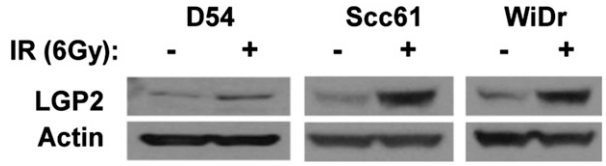

Fig. 4. LGP2 is radioinducible. D54, WiDr, and Scc61 cells were irradiated at 6 Gy; 72 h post-IR, cell lysates were analyzed by Western blotting.

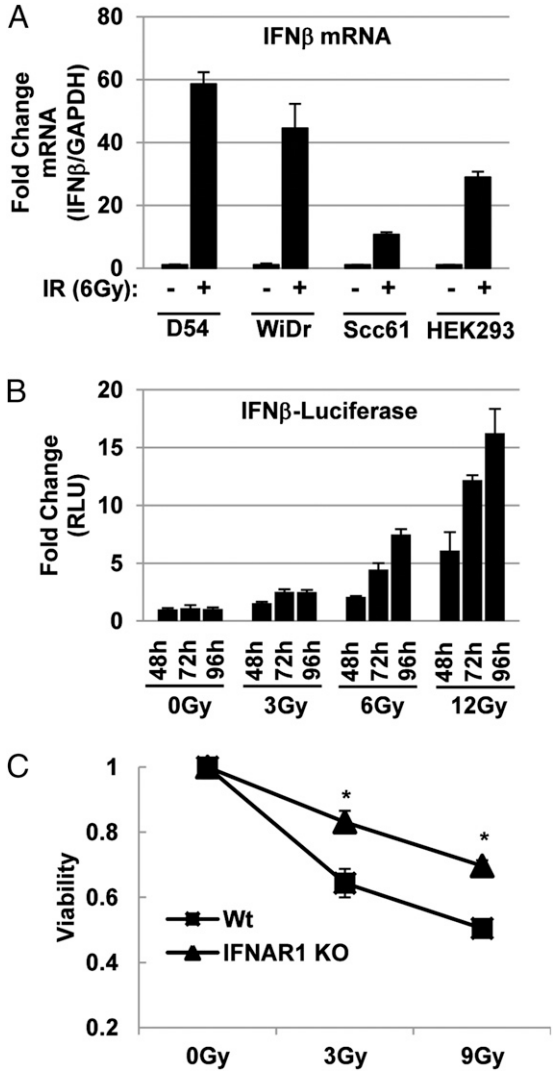

Fig. 5. IR induces cytotoxic IFNβ response. (*A*) Radiation-induced expression of IFNβ mRNA. IFNβ expression in D54, WiDr, SCC61, and HEK293 cells treated with or without 6 Gy IR was measured by qRT-PCR and normalized to GAPDH expression. Data are expressed as fold change relative to nonirradiated cells. (*B*) Radiation-induced activation of IFNβ promoter. HEK293 cells were transiently cotransfected with pGL3–Ifnβ and pRL–SV40. Firefly luciferase was normalized to *Renilla* luciferase and is expressed relative to nonirradiated cells at each collection time. (*C*) Type I IFN receptor (IFNAR1) is needed for cytotoxicity induced by IR. WT and IFNAR1$^{-/-}$ MEFs were treated with the indicated doses of IR and collected 96 h post-IR. Viability was determined by methylene blue staining and extraction, followed by spectrophotometric quantification. Viability is shown relative to nonirradiated control cells. Data are represented as means with SDs for assays performed at least in triplicate.

(Promega). This experiment was repeated to confirm reproducibility of the data. The top two siRNAs were selected for subsequent quantitative RT-PCR experiments to confirm suppression of LGP2 mRNA on the basal level and after IFNβ treatment. Based on these data, two individual siRNAs were selected and used in all subsequent experiments: 3, (5′-CCAGUACCUAGAACUUAA-3′), and 4, (5′-AGAAUGAGCUGGCCCACUU-3′).

Cell Cultures. B6 WT and B6/IFNAR1$^{-/-}$ mice were generously provided by Yang-Xin Fu at the University of Chicago (Chicago, IL) and used in accordance with the animal experimental guidelines set by the Institute of Animal Care and Use Committee. Primary MEFs were obtained from 13.5 d postcoitus embryos and cultivated in DMEM supplemented with 10% FBS, nonessential amino acids, and penicillin/streptomycin for no more than seven passages as previously described (38). MEFs were immortalized with a retrovirus expressing SV40-large T antigen (Addgene plasmid 13970) (39). Tumor cell lines used for siRNA screen and subsequent experiments were Scc61 and Nu61 (head and neck squamous cell carcinoma); D54, T98G, and U251 (GBM); WiDr and HCT116 (colorectal carcinoma); MDA–MB-231 and MCF7 (breast adenocarcinoma); MCF10a (immortalized human mammary epithelial cells); DU154 (prostate cancer); A549 and NCI–H460 (lung adenocarcinoma); and T24 (bladder cancer). Cell lines were cultivated as follows: Scc61 and Nu61 in DMEM/F12 with 20% FBS, 1% P/S (Penicillin/Streptomycin), and 1% HC (hydrocortisone); D54, T98G, and WiDr in MEM with 10% FBS and 1% P/S; U251, HCT116, MDA–MB-231, and MCF7 in DMEM high glucose with 10% FBS and 1% P/S; MCF10A MEBM (Mammary Epithelial Basal Medium) with MEGM (Mammary Epithelial Cell Growth Medium) kit (ATCC), cholera toxin (100 ng/mL), and 1% P/S; DU145 in DMEM F12 with 10% FBS and 1% P/S; A549 and NCI–H460 in RPMI with 10% FBS and 1% P/S; and T24 in McCoy's 5A AMedium with 10% FBS and 1% P/S.

Retro- and Lentiviral Production and Transduction. Retrovirus was produced using complete packaging ecotropic Plat-E cells (Cell Biolabs) by Fugene-mediated transfection of pBABE–puro SV40 LT (39). Lentivirus was produced by cotransfection of VSVG, VPR, and pLKO.1 lentiviral vector with inserted LGP2 shRNA sequence (ATTCTTGCGGTCATCGAACAG, Thermo Scientific) or

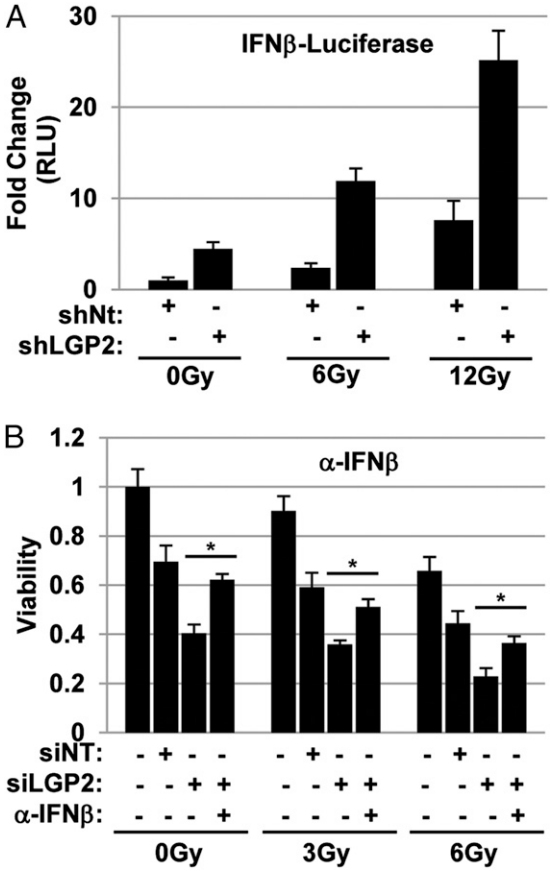

Fig. 6. LGP2 inhibits IR-induced cytotoxic IFNβ. (*A*) LGP2 suppresses IR-induced activation of IFNβ promoter. HEK293 cells were stably transduced with shRNA directed to LGP2 or shNT. Cells were transfected with pGL3–Ifnβ and pRL–SV40, irradiated (indicated dose), and collected 72 h after IR. Firefly luciferase activity was normalized to *Renilla* luciferase activity and is expressed relative to nonirradiated cells. (*B*) Neutralizing antibodies to IFNβ prevent cytotoxic effects of LGP2 depletion. D54 cells were depleted of LGP2 with siRNA (Fig. 2*C*) and irradiated at 0, 3, or 6 Gy in the presence or absence of neutralizing antibody to IFNβ (1 μg/mL). Cell viability was assessed 96 h post-IR using methylene blue assay. Data are normalized to nontargeting siRNA at 0 Gy and represented as means with error bars showing SDs for assays performed at least in triplicate. Significance was measured using two-tailed *t* test (*$P < 0.05$).

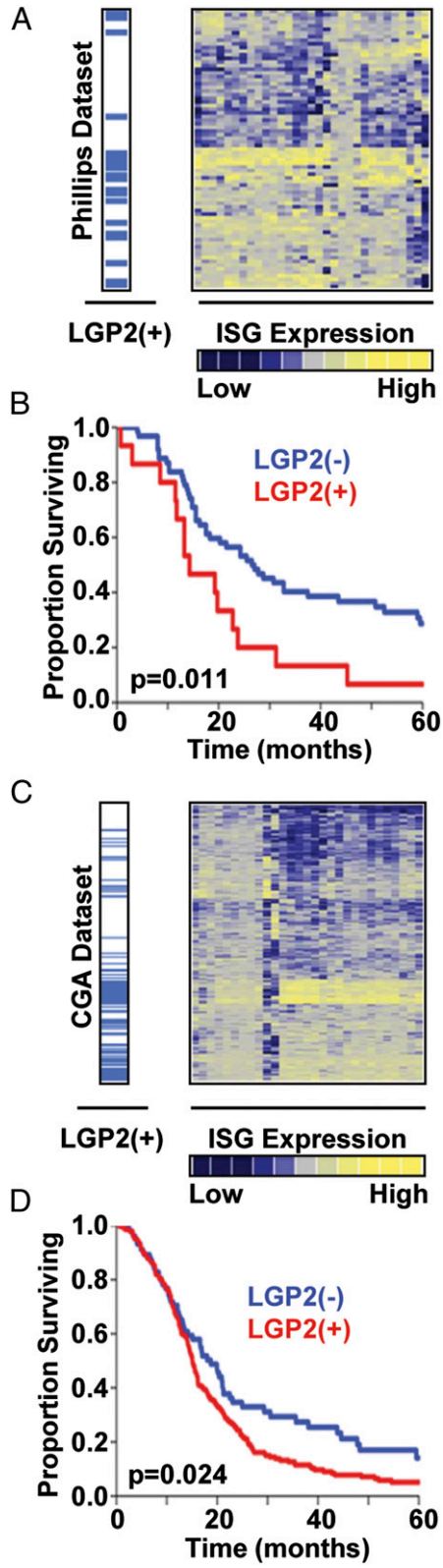

Fig. 7. Expression of LGP2 is associated with poor overall survival in patients with GBM. (*A*) Expression of ISGs and LGP2 in the Phillips database (37) (n = 77). Yellow represents up-regulated and blue down-regulated genes. Rows correspond to patients, and columns correspond to individual genes in IRDS signature (10, 13). (*B*) Kaplan–Meier survival of LGP2-high (LGP2+) and LGP2-low (LGP2–) patients from the Phillips et al. database. (*C*) Expression of ISGs and LGP2 in the TCGA database (n = 382) and (*D*) survival of LGP2+ and LGP2– patients in CGA database. *P* values represent Cox proportional hazards test.

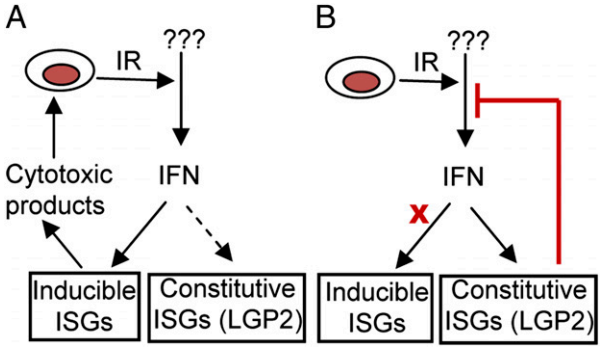

Fig. 8. Activation of IFNβ by IR is suppressed by LGP2. Acute response to IR leads to activation of IFNβ and induction of ISGs with cytotoxic functions (*A*). Chronic exposure to cytotoxic stress leads to constitutive expression of some ISGs with prosurvival functions and LGP2-dependent suppression of the autocrine IFNβ loop (*B*).

nontargeting control (Thermo Scientific) into HEK293X cells. Supernatants containing infectious viral particles were harvested 48 h posttransfection and passed through a 0.45 μm filter. Infections of exponentially growing cells were performed with virus-containing supernatant supplemented with 8 μg/mL polybrene. In lentiviral shRNA experiments, transduced cells were continually selected in the presence of puromycin (1–2 μg/mL).

Western Blotting. Western blotting was performed as described previously (2). The following antibodies were used: anti-LGP2 (sc134667; Santa Cruz) (1:1,000) and anti–Actin–HRP (Sc47778, Santa Cruz) (1:5,000). Secondary antibodies conjugated to HRP (Santa Cruz) were used at 1:10,000. Experimental findings were confirmed in at least three independent experiments.

qRT-PCR. Total RNA was extracted using TRIzol reagent (Invitrogen), treated with DNase I (Invitrogen), and reverse transcribed using SuperScript III (Invitrogen), and the cDNA products were resuspended in 20 μL of H_2O and used for PCR with Fast SYBR green master mix and a StepOnePlus real-time PCR system (both from Applied Biosystems). The following human-gene–specific primers were used: IFNβ sense primer 5′-AACTTTGACATCCCTGAG-GAGATT-3′ and antisense primer 5′-GCGGCGTCCTCCTTCTG-3′; GAPDH sense 5′-CTCTGCTCCTCCTGTTCGAC-3′ and antisense 5′-GTTAAAAGCAGCCCTGGT-GA-3′. All samples were amplified in duplicate, and every experiment was repeated independently at least two times. Relative gene expression was determined using the $2^{-\Delta\Delta CT}$ method, with GAPDH as the internal control.

Luciferase Assay. To measure IFNβ promoter activity, HEK293 cells were transiently cotransfected using Fugene (Roche) with pGL3–Ifnβ–Luc (33) and an expression plasmid carrying the *Renilla* luciferase gene driven by the SV40 promoter (Promega). In some experiments, cotransfection mixes also included p3xFLAG–CMV10–LGP2 (40) expression plasmid (or p3xFLAG–CMV10control). The following day, cells were irradiated at the indicated dose and collected at the indicated time in passive lysis buffer (Promega). Firefly and *Renilla* luciferase activities were measured using a dual-luciferase assay system (Promega). For siRNA experiments, siRNAs against LGP2 (see above) or nontargeting (Dharmacon) were transfected with RNAimax 24 h before transfection of luciferase/*Renilla* plasmids. Mean luciferase values were normalized and quantified from duplicate runs for each of at least three separate experiments.

Viability Assay. To determine cell viability, cells were plated in triplicate in 96-well plates at a density of 3,000 cells per well and treated with increasing amounts of IR. At the indicated time, cells were stained using 0.4% methylene blue in 50% methanol (41). Dye was extracted from stained cells using 3% HCl solution for spectrophotometric quantitation at 660 nm. In some experiments, neutralizing antibodies to IFNβ [Pestka Biomedical Laboratories (PBL) Assay Science, 1 μg/mL] or isotype control IgG_1 (RD Systems) were incubated with cells 1 h prior to irradiation.

Clonogenic Assay. Cells were seeded to form colonies in p60 plates and treated the next day with 1, 3, 5, or 7 Gy IR. When sufficiently large colonies with at least 50 cells were visible (~12–15 d), the plates were fixed with methanol and stained with crystal violet as previously described. Colonies with more

than 50 cells were counted, and the surviving fraction was calculated (42). For siRNAs experiments, the indicated siRNA was transfected 24 h before plating for the clonogenic assay. In overexpression experiments, D54 cells were transfected with p3xFLAG–CMV10 or p3xFLAG–CMV10–LGP2, selected in G418 for 2 wk (200 μg/mL), and individual clones were verified for stable LGP2 expression and assessed in clonogenic assays.

Flow Cytometric Analysis. Single-cell suspensions of cells were isolated and incubated with anti–Annexin V and propidium iodide according to the manufacturer's instructions (Annexin V Apoptosis Detection Kit, eBioscience). Samples were analyzed on a FACSCanto flow cytometer (BD Biosciences), and data were analyzed with FlowJo software (TreeStar, Inc.).

Statistical Analysis. ***siRNA screen analysis.*** For each of the basal-level and IR screens, the intensities of the plate were first log2 transformed and then normalized with normalized percent inhibition method to correct for plate effect. The normalized intensities were further divided by the per-plate median absolute deviations to adjust the variance. The procedures were performed using Bioconductor package cellHTS2 (43). To identify the genes that lead to the most consistent decrement in cell viability when suppressed across 14 cell lines, we conducted a rank aggregation on the gene rank lists obtained from basal-level and IR screens, separately. The Robust Rank Aggregation (RAA) algorithm implemented in R package RobustRankAggreg was applied (44). Briefly, the RRA method assumes a null model where the ranks of each gene are uniformly distributed over the rank lists. For each plate, the 89 genes were sorted in descending order of their median normalized intensity of the three replicates. Then for each position in the sorted list, the probability that a randomly sampled rank from the null model has a lower rank value than the value at that position in the sorted list can be calculated. The minimum of the resulting probabilities over all positions in the sorted list is defined as the rank score of the gene, which can then be converted into an estimated *P* value of the gene through Bonferroni correction (45). The derived *P* values are subject to multiple testing correction to control the false discovery rate (FDR) by Benjamini–Hochberg procedure (46). To further evaluate the stability of Bonferroni-corrected *P* values, we applied a leave-one-out permutation test on the RRA algorithm (47). The analysis was conducted by performing RRA on a subset of 14 gene lists with one randomly selected list excluded. The procedure was repeated 100,000 times, and the *P* values from each permutation for each gene were then averaged.

Database analysis. Glioblastoma datasets were collected from the CGA (n = 382) and Phillips et al. study (n = 77) (37). Only patients with a history of prior radiation therapy were included in the analysis. mRNA expression values were normalized to the median value across all patient samples within each respective dataset. Gene expression data were visualized using hierarchical clustering. ISG expression was based on the mRNA expression of IFN-inducible genes as reviewed in ref. 10. Kaplan–Meier survival analysis with a log-rank test was used to compare overall survival for LGP2-positive patients, defined as 1.5-fold increased expression above the group median, versus LGP2-negative patients. Cox proportional hazard analysis of overall survival was performed to determine the hazard ratio for overall survival of LGP2-positive versus LGP2-negative patients. All analyses were performed using JMP 9.0 (SAS Institute Inc.). A P value ≤ 0.05 was considered statistically significant.

Quantitative data analysis. Data are presented as means ± SDs for three or more representative experiments. Statistical significance was calculated using Student t test.

ACKNOWLEDGMENTS. We gratefully acknowledge Dr. Samuel Hellman and Dr. Byron Burnette (University of Chicago) for helpful discussion of the manuscript; Dr. Samuel Bettis, Dr. Siquan Chen, and Rita Grantner (Cell Screening Center, University of Chicago) for assistance with siRNA screen; Dr. Yang-Xin Fu (University of Chicago) for generously providing B6/IFNAR1 KO (IFN receptor type 1 knockout) mice; and Drs. Curt M. Horvath (Northwestern) and Michael Gale, Jr. (University of Washington) for generously providing LGP2 constructs. This work was supported in part by the Ludwig Center for Metastasis Research Grant, the Center for Radiation Therapy, the Chicago Tumor Institute, the Ludwig Foundation for Cancer Research, Mr. and Mrs. Vincent Foglia and the Foglia Foundation, Lung Cancer Research Foundation, the Cancer Research Foundation, and National Institutes of Health Grants R0-1 CA111423 and PO1-CA71933 (to R.R.W.).

1. Khodarev NN, et al. (2004) STAT1 is overexpressed in tumors selected for radioresistance and confers protection from radiation in transduced sensitive cells. *Proc Natl Acad Sci USA* 101(6):1714–1719.
2. Khodarev NN, et al. (2007) Signal transducer and activator of transcription 1 regulates both cytotoxic and prosurvival functions in tumor cells. *Cancer Res* 67(19):9214–9220.
3. Tsai MH, et al. (2007) Gene expression profiling of breast, prostate, and glioma cells following single versus fractionated doses of radiation. *Cancer Res* 67(8):3845–3852.
4. John-Aryankalayil M, et al. (2010) Fractionated radiation therapy can induce a molecular profile for therapeutic targeting. *Radiat Res* 174(4):446–458.
5. Cheon H, Yang J, Stark GR (2011) The functions of signal transducers and activators of transcriptions 1 and 3 as cytokine-inducible proteins. *J Interferon Cytokine Res* 31(1): 33–40.
6. Amundson SA, et al. (2004) Human in vivo radiation-induced biomarkers: Gene expression changes in radiotherapy patients. *Cancer Res* 64(18):6368–6371.
7. Borden EC, et al. (2007) Interferons at age 50: Past, current and future impact on biomedicine. *Nat Rev Drug Discov* 6(12):975–990.
8. Samuel CE (2001) Antiviral actions of interferons. *Clin Microbiol Rev* 14(4):778–809.
9. Kotredes KP, Gamero AM (2013) Interferons as inducers of apoptosis in malignant cells. *J Interferon Cytokine Res* 33(4):162–170.
10. Khodarev NN, Roizman B, Weichselbaum RR (2012) Molecular pathways: Interferon/stat1 pathway: Role in the tumor resistance to genotoxic stress and aggressive growth. *Clin Cancer Res* 18(11):3015–3021.
11. Perou CM, et al. (1999) Distinctive gene expression patterns in human mammary epithelial cells and breast cancers. *Proc Natl Acad Sci USA* 96(16):9212–9217.
12. Perou CM, et al. (2000) Molecular portraits of human breast tumours. *Nature* 406(6797):747–752.
13. Weichselbaum RR, et al. (2008) An interferon-related gene signature for DNA damage resistance is a predictive marker for chemotherapy and radiation for breast cancer. *Proc Natl Acad Sci USA* 105(47):18490–18495.
14. Martin DN, Starks AM, Ambs S (2013) Biological determinants of health disparities in prostate cancer. *Curr Opin Oncol* 25(3):235–241.
15. Duarte CW, et al. (2012) Expression signature of IFN/STAT1 signaling genes predicts poor survival outcome in glioblastoma multiforme in a subtype-specific manner. *PLoS ONE* 7(1):e29653.
16. Hix LM, et al. (2013) Tumor STAT1 transcription factor activity enhances breast tumor growth and immune suppression mediated by myeloid-derived suppressor cells. *J Biol Chem* 288(17):11676–11688.
17. Haricharan S, Li Y (2014) STAT signaling in mammary gland differentiation, cell survival and tumorigenesis. *Mol Cell Endocrinol* 382(1):560–569.
18. Camicia R, et al. (2013) BAL1/ARTD9 represses the anti-proliferative and pro-apoptotic IFNγ-STAT1-IRF1-p53 axis in diffuse large B-cell lymphoma. *J Cell Sci* 126(Pt 9): 1969–1980.
19. Cheon H, et al. (2013) IFNβ-dependent increases in STAT1, STAT2, and IRF9 mediate resistance to viruses and DNA damage. *EMBO J* 32(20):2751–2763.
20. Malur M, Gale M, Jr., Krug RM (2012) LGP2 downregulates interferon production during infection with seasonal human influenza A viruses that activate interferon regulatory factor 3. *J Virol* 86(19):10733–10738.
21. Komuro A, Horvath CM (2006) RNA- and virus-independent inhibition of antiviral signaling by RNA helicase LGP2. *J Virol* 80(24):12332–12342.
22. Akira S, Uematsu S, Takeuchi O (2006) Pathogen recognition and innate immunity. *Cell* 124(4):783–801.
23. Kawasaki T, Kawai T, Akira S (2011) Recognition of nucleic acids by pattern-recognition receptors and its relevance in autoimmunity. *Immunol Rev* 243(1):61–73.
24. Multhoff G, Radons J (2012) Radiation, inflammation, and immune responses in cancer. *Front Oncol* 2:58.
25. Suthar MS, et al. (2012) The RIG-I-like receptor LGP2 controls CD8(+) T cell survival and fitness. *Immunity* 37(2):235–248.
26. Khodarev NN, et al. (2009) STAT1 pathway mediates amplification of metastatic potential and resistance to therapy. *PLoS ONE* 4(6):e5821.
27. Adler P, et al. (2009) Mining for coexpression across hundreds of datasets using novel rank aggregation and visualization methods. *Genome Biol* 10(12):R139.
28. Boulesteix AL, Slawski M (2009) Stability and aggregation of ranked gene lists. *Brief Bioinform* 10(5):556–568.
29. Saito T, et al. (2007) Regulation of innate antiviral defenses through a shared repressor domain in RIG-I and LGP2. *Proc Natl Acad Sci USA* 104(2):582–587.
30. Yoneyama M, et al. (2005) Shared and unique functions of the DExD/H-box helicases RIG-I, MDA5, and LGP2 in antiviral innate immunity. *J Immunol* 175(5):2851–2858.
31. Komuro A, Bamming D, Horvath CM (2008) Negative regulation of cytoplasmic RNA-mediated antiviral signaling. *Cytokine* 43(3):350–358.
32. Rothenfusser S, et al. (2005) The RNA helicase Lgp2 inhibits TLR-independent sensing of viral replication by retinoic acid-inducible gene-I. *J Immunol* 175(8):5260–5268.
33. Lin R, Génin P, Mamane Y, Hiscott J (2000) Selective DNA binding and association with the CREB binding protein coactivator contribute to differential activation of alpha/beta interferon genes by interferon regulatory factors 3 and 7. *Mol Cell Biol* 20(17): 6342–6353.
34. Walker MD, et al. (1978) Evaluation of BCNU and/or radiotherapy in the treatment of anaplastic gliomas. A cooperative clinical trial. *J Neurosurg* 49(3):333–343.
35. Kristiansen K, et al. (1981) Combined modality therapy of operated astrocytomas grade III and IV. Confirmation of the value of postoperative irradiation and lack of potentiation of bleomycin on survival time: A prospective multicenter trial of the Scandinavian Glioblastoma Study Group. *Cancer* 47(4):649–652.
36. Laperriere N, Zuraw L, Cairncross G; Cancer Care Ontario Practice Guidelines Initiative Neuro-Oncology Disease Site G (2002) Radiotherapy for newly diagnosed malignant glioma in adults: A systematic review. *Radiother Oncol* 64(3):259–273.

37. Phillips HS, et al. (2006) Molecular subclasses of high-grade glioma predict prognosis, delineate a pattern of disease progression, and resemble stages in neurogenesis. *Cancer Cell* 9(3):157–173.
38. Widau RC, et al. (2012) p19Arf represses platelet-derived growth factor receptor β by transcriptional and posttranscriptional mechanisms. *Mol Cell Biol* 32(21):4270–4282.
39. Zhao JJ, et al. (2003) Human mammary epithelial cell transformation through the activation of phosphatidylinositol 3-kinase. *Cancer Cell* 3(5):483–495.
40. Bamming D, Horvath CM (2009) Regulation of signal transduction by enzymatically inactive antiviral RNA helicase proteins MDA5, RIG-I, and LGP2. *J Biol Chem* 284(15): 9700–9712.
41. Leonova KI, et al. (2013) p53 cooperates with DNA methylation and a suicidal interferon response to maintain epigenetic silencing of repeats and noncoding RNAs. *Proc Natl Acad Sci USA* 110(1):E89–E98.
42. Mauceri HJ, et al. (1998) Combined effects of angiostatin and ionizing radiation in antitumour therapy. *Nature* 394(6690):287–291.
43. Boutros M, Brás LP, Huber W (2006) Analysis of cell-based RNAi screens. *Genome Biol* 7(7):R66.
44. Kolde R, Laur S, Adler P, Vilo J (2012) Robust rank aggregation for gene list integration and meta-analysis. *Bioinformatics* 28(4):573–580.
45. Dunn OJ (1961) Multiple comparisons among means. *J Am Stat Assoc* 56(293): 52–64.
46. Benjamini Y, Hochberg Y (1995) Controlling the false discovery rate—A practical and powerful approach to multiple testing. *J Roy Stat Soc B Met* 57(1):289–300.
47. Võsa U, et al. (2013) Meta-analysis of microRNA expression in lung cancer. *Int J Cancer* 132(12):2884–2893.